Homogeneous and compact acoustic ground cloaks

Bogdan-Ioan Popa* and Steven A. Cummer†
Department of Electrical and Computer Engineering, Duke University, Durham, North Carolina 27708, USA
(Received 31 January 2011; revised manuscript received 8 April 2011; published 24 June 2011)

We present the design, architecture, and detailed performance predictions for a class of ground-plane acoustic cloaking shells. The design begins with a coordinate transformation which, in contrast to a quasiconformal design, yields a homogeneous but anisotropic material and a shell size that is comparable to the size of the object to be hidden. We apply the general approach to the design of a broadband acoustic cloak in water, in which the desired material parameters are realized through acoustic metamaterials composed of blocks of steel, aluminum foam, and silicon carbide foam. Since metallic and ceramic foams are prone to sound absorption, we discuss the effects of loss inside the two types of foam. An important part of this design consists in reducing the shear wave effects inside the solids by isolating these solids from each other through narrow channels of background fluid. Numerical simulations of the entire device, as composed of the discrete and basic material building blocks, demonstrates good performance and shows that such a device can be physically realized through the assembly of available materials in a relatively simple form.

DOI: 10.1103/PhysRevB.83.224304 PACS number(s): 46.40.Cd

I. INTRODUCTION

Coordinate transformations provide a powerful technique to design devices capable of remarkable control over wave propagation. The concept was proposed initially for electromagnetic waves,[1,2] and later extended to acoustics.[3] One of the most remarkable applications enabled by this technique was the so called "invisibility cloak" (or simply "cloak"), a coating shell able to completely cancel the scattering of incident waves off objects surrounded by the coating. This application was extensively analyzed in the context of both electromagnetics.[1,2,4–9] and acoustics[3,10–14] Such analysis revealed the main difficulties encountered when trying to implement cloaking devices: they have to be inhomogeneous (i.e., the material parameters have to vary continuously with position) and very anisotropic. One notable implementation of a cloaking acoustic device in water has recently been reported[15] and emphasizes these challenges.

Subsequent research lead to the concept of "ground cloak,"[16] i.e., a device covering objects positioned on a reflecting surface that cancels the scattering off the objects themselves, thus rendering the objects indistinguishable from the reflecting surface. The ground cloak proved easier to realize in practice due to its property that it can be generated through quasiconformal mappings, and therefore the anisotropy can be minimized inside the coating.[16] This approach has been taken in order to demonstrate the concept experimentally for electromagnetic waves in both microwave[17] and optical[18–20] domains but not for acoustics. As pointed out in these experiments, one disadvantage of the quasiconformal ground cloak is its large size: it typically needs to be an order of magnitude larger than the object it is designed to hide. The other disadvantage is the cloak inhomogeneity which translates into a complex design and fabrication process.

Here, we describe and apply a design approach that addresses these disadvantages. We allow a reasonably small amount of anisotropy in exchange for homogeneity and compact designs. We show that this approach applied to acoustic ground cloaks leads to practical (i.e., relatively easy to fabricate), broadband designs for transformation acoustics devices that can be realized essentially without approximations. We demonstrate our method by designing a realizable acoustic "ground cloak" and investigate its effectiveness through numerical simulations of the realizable ground cloak. An important part of our design consists in using metal and/or ceramic foams to control the effective material parameters inside the device. Since these materials are prone to sound absorption, we also discuss the effects of power loss inside the foams to cloaking performance.

The simulations are performed with the "Acoustic-Structure Interaction" application mode of Comsol Multiphysics which takes into account the elastodynamics of the solid device components. As pointed out in the past,[21,22] the shear wave phenomena in solids are detrimental to transformation acoustics devices because the full elastodynamics equations are not transformation invariant. We describe a technique later in the paper that allows a significant reduction of shear wave effects, so that the acoustic metamaterials presented here have negligible effective shear moduli, and the relevant effective material parameters involved in the design are the mass density tensor and scalar bulk modulus.

II. DESIGN METHOD

Figure 1 illustrates our method to obtain homogeneous ground cloaks. The object that needs to be hidden has a triangular shape. The coordinate transformation technique requires us to find mapping functions that map the space occupied by the object to the surface of the reflector. We call the space of the object the "real space" (described by the x and y Cartesian coordinates), and the transformed space in which the object is reduced to a flat surface the "virtual space" (described by the u and v coordinates). The region affected by the these mapping functions, i.e., the region occupied by the cloak in the real space, is represented by the shaded regions inside the dotted line shown in Fig. 1. We will discuss shortly how we choose the cloak geometry and size.

Since the material parameters inside the cloak are given by the first partial derivatives of the transformation functions,

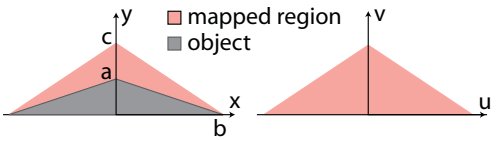

FIG. 1. (Color online) Principle behind the ground cloak. A mapping between the real, xy, and virtual, uv, spaces is chosen such that the object in the real space is flattened, i.e., mapped to the ground plane, in the virtual space

in order to obtain a homogeneous cloak, we require the transformation functions to be linear. One such choice suitable for the triangular object considered here is

$$\begin{aligned} u &= x, \\ v &= \frac{c}{c-a}\left(-a + \frac{a}{b}|x| + y\right), \\ w &= z, \end{aligned} \tag{1}$$

where a and b are given by the geometry of the object, and c is a parameter that determines the height of the cloak. Similar linear transformations were considered in Refs. 23–25 for different applications. The isocontours of the mapping functions u (vertical blue lines) and v (horizontal red lines) are illustrated in Fig. 3(a).

We note that the expression of v is not linear inside the whole transformation domain; however, it is linear inside each one of the $x < 0$ and $x > 0$ domains. This translates into same material parameters in each half of the cloak but different directions of the principal axis, defined as the directions along which the material parameter tensors are diagonal.

According to the coordinate transformation theory,[3] the mapping functions given by Eq. (1) translate to the following material parameters:

$$\begin{aligned} \overline{\overline{\rho}} &= \begin{pmatrix} \frac{c-a}{c} + \frac{c}{c-a}\left(\frac{a}{b}\right)^2 & -\text{sign}(x)\frac{ac}{b(c-a)} \\ -\text{sign}(x)\frac{ac}{b(c-a)} & \frac{c}{c-a} \end{pmatrix}, \\ B &= \frac{c-a}{c}. \end{aligned} \tag{2}$$

The above matrix can be diagonalized by a suitable rotation of the xyz coordinate system around the off-plane z axis. The rotated system of coordinates is called the principal system, and the two non-zero components of the diagonalized density matrix are given by the eigenvalues of $\overline{\overline{\rho}}$. Written in the principal system, the above material parameters become

$$\begin{aligned} \overline{\overline{\rho}}_{pr} &= \begin{pmatrix} F + \sqrt{F^2-1} & 0 \\ 0 & F - \sqrt{F^2-1} \end{pmatrix}, \\ B_{pr} &= \frac{c-a}{c}, \end{aligned} \tag{3}$$

where

$$F = 1 + \frac{a^2(b^2+c^2)}{2b^2c(c-a)}. \tag{4}$$

From a practical point of view, Eq. (3) gives the physical effective material parameters of the material needed to implement the cloak. Moreover, the material has to be aligned with the axis of the principal system. The rotation angle that gives the direction of the principal system relative to the orientation of the xyz system is determined from the eigenvectors of $\overline{\overline{\rho}}$ [see Eq. (2)], and can be expressed as

$$\alpha = \text{sign}(x)\arcsin\left(\frac{G}{1+\sqrt{G^2}}\right), \tag{5}$$

where

$$G = \frac{b}{c}\left[1 - \frac{c-a}{a}(F - 1 - \sqrt{F^2-1})\right]. \tag{6}$$

Equations. (3) and (5) are typical design equations for the homogeneous ground cloak. We notice that, unlike most cloak designs reported in the literature, the material parameters are constant with position throughout the cloak. This implies that, in order to fabricate such a device, only one type of metamaterial composite is required. Moreover, unlike quasiconformal cloaks[16] which need to be much more voluminous than the object they hide, our cloak can be made very thin, depending on the degree of anisotropy we can achieve inside the metamaterial used to implement the cloak.

III. EXAMPLE OF CLOAK IMPLEMENTATION

Next we illustrate these advantages by designing a realizable acoustic cloak made of commercially available materials, and show its performance in numerical simulations. The background fluid is water of density $\rho_0 = 1000$ kg/m^3 and bulk modulus $B_0 = 2.25$ GPa. All material parameters given below will be relative to the parameters of water. As an example, we require the cloak to work below 1500 Hz, or equivalently at wavelengths greater than 1 m.

The triangular object is characterized by $a = 0.5$ m and $b = 1.5$ m. We choose the object and cloak height to be $c = 1$ m, which result in a cloak volume equal to the volume of the object, i.e., an order of magnitude less voluminous than a typical quasiconformal cloak. We chose an object that is three wavelengths in diameter at the highest working frequency in order to simplify the complexity of the numerical simulations. It is important to note that the metamaterial design (i.e., more specifically the metamaterial unit cell, as we will see shortly) does not depend on the object size as long as the ratio $a : b : c$ remains the same. This means that objects of arbitrary size can be cloaked using the same design presented below.

From Eqs. (3) and (5), the material parameters inside the cloak written in the principal system, and the rotation angle of the principal system become

$$\overline{\overline{\rho}}_{pr} = \begin{pmatrix} 2.28 & 0 \\ 0 & 0.44 \end{pmatrix}, \quad B_{pr} = 0.5, \quad \alpha = \text{sign}(x) \times 66.9^\circ. \tag{7}$$

We notice that the required material parameters are relatively close to those of water, well within achievable limits. In the same time, the anisotropy factor, defined as the ratio of the diagonal terms of $\overline{\overline{\rho}}_{pr}$ in Eq. (7), i.e., $\rho_{pr}^{(11)}/\rho_{pr}^{(22)} = 5.2$, remains relatively low, obtainable in acoustic metamaterials. It has been shown that such anisotropy is available in metamaterials composed of layers of isotropic materials,[12] solid inclusions in a background fluid,[26,27] or perforated solid plates.[28] Due to its generality and since its effectiveness has already been demonstrated in numerical simulations, we chose the approach

of Ref. 27; however, we emphasis that any of the above-mentioned metamaterial architectures is a feasible option and may even prove easier to implement in practice.

The less than unity mass density and modulus are typical for metal foams used in underwater acoustics applications. In our design, we use aluminum foam[29] characterized by a Young's modulus of 0.7 GPa, density 160 kg/m^3, and Poisson's ratio 0.27, as well as silicon carbide foam[30] (Young's modulus 2.79 GPa, density 160 kg/m^3, and Poisson's ratio 0.22). The denser than water material needed to obtain the higher component of the $\overline{\overline{\rho}}_{pr}$ tensor is steel (Young's modulus 113 GPa, density 7910 kg/m^3, and Poisson's ratio 0.33). Although two type of materials (steel and one type of aluminum foam) is enough in order to obtain an acoustic metamaterial characterized by the effective parameters given in Eq. (7), we used three different types of materials in order to illustrate the method in a more complex setting.

Using the technique described in detail in Ref. 27, we designed a highly subwavelength square unit cell having 5 cm edges, i.e., it is smaller than the wavelength at the highest frequency of 1500 Hz by a factor of 20. As pointed out before,[27] a metamaterial generated by this cell approximates well a homogeneous material characterized by effective density and bulk modulus. The accuracy of this approximation will be demonstrated in numerical simulations below.

Figure 2(b) shows the structure of the unit cell including all the relevant dimensions that give effective parameters within 3% of these specified by Eq. (7), i.e., $\rho_{pr}^{(11)} = 2.28$, $\rho_{pr}^{(22)} = 0.43$, and $B_{pr} = 0.5$. The solid particles composing the unit cell are surrounded from all sides by liquid in order to reduce the subwavelength effects of the shear waves in the solids. The same Fig. 2(b) illustrates the cloak implementation using the unit cell. The orientation of the unit cell axis is given by the rotation angle of the principle system as specified in Eq. (7), i.e., $\alpha = \text{sign}(x) \times 66.9^\circ$. We note that the cell geometry and size does not allow the metamaterial to fully fill the theoretical volume of the cloak. Since it provides good results, we chose a simple filling strategy in which the cloak involves only square unit cells which do not cross the boundaries of the theoretical cloaking domain. Other filling strategies are, however, possible, including ones involving the design of triangular unit cells for the volume left uncovered.

The asymmetric geometry of the two halves of the cloak is the result of the particular algorithm used in this filling strategy, and it is not an essential characteristic for the design performance. A symmetric cloak would provide a very similar behavior to the one presented here.

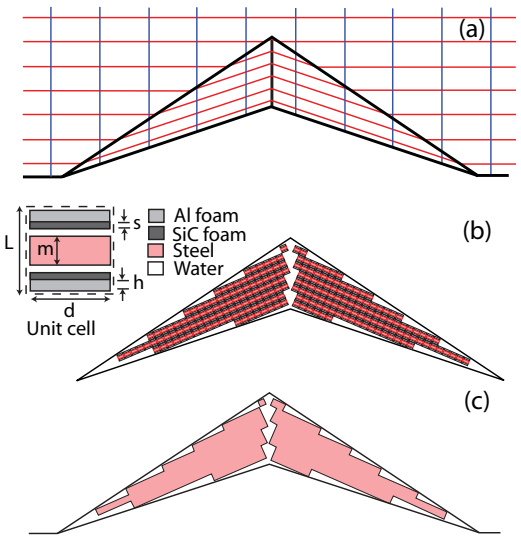

FIG. 2. (Color online) Ground cloak design. (a) Contour plot of mapping functions $u(x)$ and $v(x,y)$; (b) structure of cloak composed of arrays of discrete unit cells. The dimensions of the unit cell elements are $L = 50$ mm, $d = 47.5$ mm, $m = 14.7$ mm, $s = 1.8$ mm, and $h = 12.38$ mm; (c) ideal cloak made of the homogeneous continuous and anisotropic material that is implemented through the metamaterial depicted at (b).

IV. RESULTS

Figure 3 shows the performance of our design obtained in numerical simulations performed with the Acoustic-Structure Interaction application mode of Comsol Multiphysics.

Figure 3(a) illustrate the ideal case: a Gaussian beam of frequency 1500 Hz propagating from left to right is incident at 45° on a rigid ground plane. The field distribution is identical to that obtained in the presence of an ideal cloak (not shown) whose material parameters are specified by Eq. (7) and that fills the entire volume of the cloak.

Figure 3(b) shows the same beam scattered by the triangular object. We notice its acoustic signature, i.e., two distinct scattered beams at ≈20° and 80°.

If the ideal cloaking material does not fill the entire ideal volume, but only the fraction presented in Fig. 2(c) that can be covered by square unit cells, then this signature is greatly reduced [see Fig. 3(c), our target behavior]. In fact, the imperfect filling has a very small effect on the device performance, namely the reflected beam in Fig. 3(c) is only slightly wider than the ideal case of Fig. 3(a) in which the ideal cloak occupies the entire volume.

Figure 3(d) shows that the metamaterial-based implementation of the cloak, whose geometry is presented in Fig. 2(b), behaves remarkably similar to the target theoretical cloak of Fig. 3(c). This good match confirms the effectiveness of the design technique presented here, and also demonstrates that efficient acoustic ground cloaks are not only physically realizable but also of relatively low complexity. We reiterate that an even better cloaking performance is possible by filling the small gap left between the two halves of the device with metamaterials designed for that particular gap geometry.

Figure 3(e) shows the same good cloak behavior while the Gaussian beam is incident under a different angle (i.e., 60°). The broadband nature of the design is demonstrated in Fig. 3(e), which illustrates the cloak effectiveness at 1000 Hz, i.e., at a frequency 33% lower than the frequency of Figs. 3(a)–3(e). In both these latter cases, the field distribution between the theoretical cloak of Fig. 3(c) and its metamaterial implementation are almost identical.

From a practical point of view, the cloak performance is usually quantified through its far-field scattering characteristics. Figure 4 shows the reflected pressure amplitude obtained seven wavelengths away from the scattering objects analyzed in Figs. 3(a)–3(d), respectively. As in these cases,

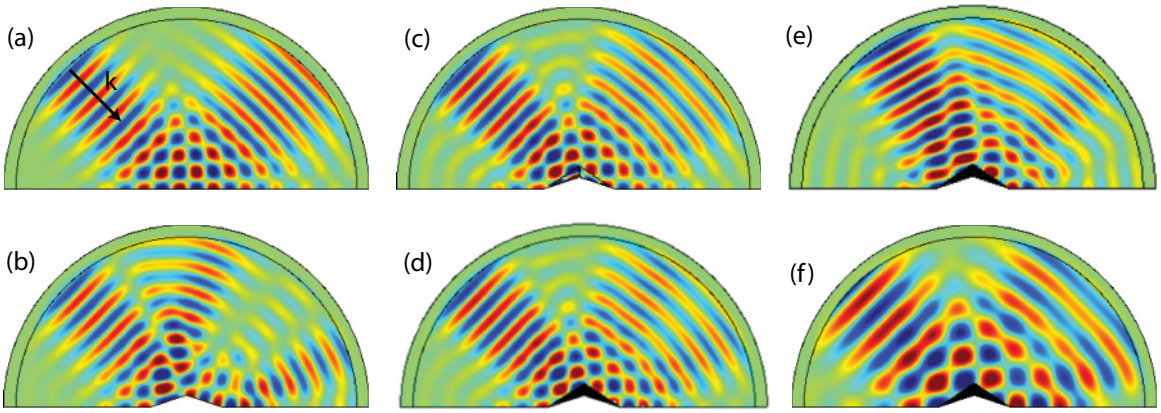

FIG. 3. (Color online) Simulated acoustic fields: (a) Gaussian beam at 1500 Hz incident at 45° on the ground reflector in the absence of the object; (b) scattering of the triangular, rigid object; (c) field distribution around the theoretical cloak of Fig. 2(c), which partially fills the theoretical cloaking domain; (d) field distribution around the metamaterial implementation of the ideal cloak; (e) Same as (d), the incident angle is 60°; and (f) same as (d), the Gaussian beam frequency is 1000 Hz.

the incoming wave is a Gaussian beam traveling under a 45° angle, and whose frequency band is centered around 1500 Hz. As expected, the pressure scattered by the ground plane [curve (a)] has a Gaussian shape centered at the incident angle of 45°. The reflection from the triangular object [curve (b)] features two lobes at 20° and 80° in agreement with Fig. 3(b).

In contrast, the target theoretical cloak we wish to implement [curve (c)], which is characterized by ideal material parameters but imperfect volume filling, generates a reflection that maintains the desired Gaussian shape. However, the incomplete filling of the ideal cloak region flattens the tip of the Gaussian, as illustrated in Fig. 4(c). The physical device obtained from blocks of metal and metal foam [curve (d)] closely follows this target behavior. The difference between curves (c) and (d) gives a measure of the effectiveness of the metamaterial approximation of the ideal material parameters.

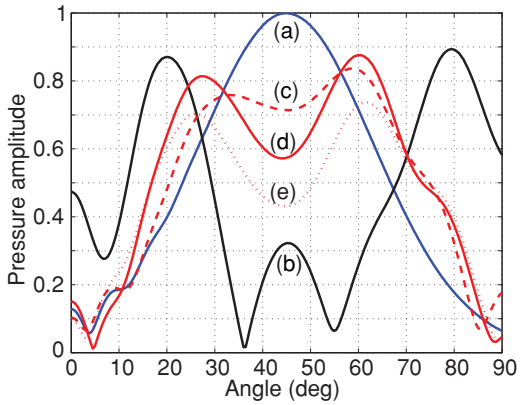

FIG. 4. (Color online) Far field pressure amplitude of the reflected sound wave measured seven wavelengths away from the target: (a) in the absence of the triangular object, i.e., ideal behavior; (b) with the object by itself; (c) with the object covered by the target theoretical cloak made of a homogeneous, continuous material whose material parameters are given by Eq. (7). The difference between this case and curve (a) is due to the ideal cloaking material filling only the fraction shown in Fig. 2(c) of the ideal volume; (d) with the object covered by the physical cloak. The difference between (c) and (d) measures the effectiveness of the metamaterial approximation of the ideal parameters we want to obtain inside the device; and (e) when the loss factor inside the two foams is 0.1 (see text).

As mentioned in Sec. III, we obtain less than unity components of the mass density tensor and bulk modulus inside the cloak by using aluminum and silicon carbide foams. Depending on the manufacturing technology, these porous materials are prone to sound absorption, which has, typically, a negative impact on the cloaking performance. A standard way to account for material losses in numerical simulations (also the approach taken by Comsol Multiphysics) is to introduce a loss factor, η, in the stress-strain relation solved inside the two foams, i.e., $\sigma = C(1 + j\eta)\epsilon$, where σ, ϵ and C are the stress, strain, and, respectively, elasticity tensors, and $j = \sqrt{-1}$.

Curve (e) in Fig. 4 shows the far field behavior when a large loss factor of 0.1 is considered. We notice that foams characterized by high damping lead to a certain attenuation of the waves that pass through the device. More importantly, however, the cloak acoustic signature, i.e., the shape of the far field distribution, depends very little on loss. This is not very surprising if we take into account that the phase velocity inside the device is not affected by damping, and also that the homogeneous structure of the design leads to constant damping throughout the cloak.

V. TECHNIQUE TO REDUCE SHEAR EFFECTS

Urzhumov *et al.*[22] showed that the coupling between the pressure and shear waves in cloaks made of continuous layers of solids characterized by large shear moduli cancels the cloaking effect. The small difference between the obtained [curve (d)] and target [curve (c)] behaviors of our design, which are mainly caused by these elastodynamic effects, shows that shear wave phenomena have minimal impact on device performance if the solid materials are divided into small pieces isolated from each other by small channels filled with fluids. Below we explain why this is the case.

Figure 5 presents the simulated velocity fields inside two types of cells excited by an acoustic plane wave propagating horizontally from left to right. The simulation domain is

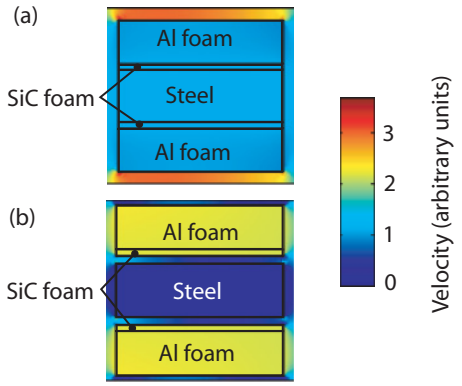

FIG. 5. (Color online) Particle velocity inside the solid inclusions for two types of unit cells: (a) foam and steel inclusions are in direct contact; (b) foam and steel inclusions are isolated by a narrow water channel. This cell was used to generate the cloak.

bounded by top and bottom periodic boundary conditions in the transverse direction, and by reflectionless perfectly matched layers in the propagation direction.

Figure 5(a) shows the simulated cell behavior if all the solid inclusions are directly connected. In spite of the fact that steel has a much larger mass than either metal foam used, the shear stress in the solids causes the particles in the steel inclusion to match their velocity to that of the surrounding foam. This leads to a large average momentum density inside the cell. Since the relevant, horizontal component of the effective mass density tensor is given by

$$\rho^{(h)} = \frac{\langle u_h \rangle}{\langle v_h \rangle} \rho_0^{-1}, \tag{8}$$

where ρ_0 is the absolute water mass density (i.e., the reference density), $\langle u_h \rangle$ and $\langle v_h \rangle$ are the horizontal components of the momentum density and, respectively, particle velocity averaged across the unit cell volume, this large momentum density translates in a big value of $\rho^{(22)}$. More specifically, the simulation gives $\rho^{(22)} = 2.5$, which is comparable to $\rho^{(11)} = 2.31$. Thus, the shear stress almost cancels the cell anisotropy, and with it the cloaking effect.

The solution to this unwanted phenomenon is to isolate the steel and foam inclusions by a small channel of background fluid as was the case of the cell used to generate the ground cloak described above. In this situation, illustrated in Fig. 5(b), the steel and metal foam particles move independently of each other, so that the velocity of the steel particles is about an order of magnitude smaller than that of the metal foams and water. This translates, according to Eq. (8), into an effective density tensor component much smaller than that of the first cell. This time $\rho^{(22)} = 0.43$ and the anisotropy of the cell is preserved along with the cloaking effect of the device generated from the cell. This parameter is within 15% of what we obtained in simulations of the same unit cell in which the shear modulus inside the solids was set to zero by replacing the steel and foam particles with fictitious fluids that had the corresponding density and bulk modulus.

VI. CONCLUSIONS

We demonstrated a procedure to obtain physically realizable homogeneous ground cloaks. The device was based on the transformation acoustics technique in which we used only linear mappings. The main advantage of this choice is the relatively low complexity of the design, which requires only one type of metamaterial unit cell, but does not sacrifice cloaking efficiency. The second advantage is the compactness of the device made possible by the anisotropy of the material composing it.

The metamaterial demonstrated here consists of sheets of steel and two types of metal and ceramic foams segmented at periodical highly subwavelength intervals, and isolated from each other through narrow channels of background fluid. We showed that this isolation is an effective way to reduce the shear wave effects inside the cloak, which are known to cancel the cloaking effect.

The good cloaking efficiency of the metamaterial implementation of this device was shown in full-wave numerical simulations of the realizable structure. Remarkably, the behavior of the cloaking structure matched very well that of the target theoretical device described by the material parameters obtained directly from the transformation acoustics equations.

In addition, we showed that sound damping inside the foam materials prone to higher absorption levels results in a certain level of attenuation that depends on the quality of the foams, but has very little effect on the acoustic signature of the cloak. The effectiveness of this design technique recommends it as a viable method to realize physical acoustic cloaks.

*bap7@ee.duke.edu
†cummer@ee.duke.edu

[1] J. B. Pendry, D. Schurig, and D. R. Smith, Science **312**, 1780 (2006).
[2] U. Leonhardt, Science **312**, 1777 (2006).
[3] S. A. Cummer and D. Schurig, New J. Phys. **9**, 45 (2007).
[4] D. Schurig, J. J. Mock, B. J. Justice, S. A. Cummer, J. B. Pendry, A. F. Starr, and D. R. Smith, Science **314**, 977 (2006).
[5] S. A. Cummer, B.-I. Popa, D. Schurig, D. R. Smith, and J. B. Pendry, Phys. Rev. E **74**, 036621 (2006).
[6] H. Chen, B.-I. Wu, B. Zhang, and J. A. Kong, Phys. Rev. Lett. **99**, 063903 (2007).
[7] W. Cai, U. K. Chettiar, A. V. Kildishev, V. M. Shalaev, and G. W. Milton, Appl. Phys. Lett. **91**, 111105 (2007).
[8] Y. Huang, Y. Feng, and T. Jiang, Opt. Express **15**, 11133 (2007).
[9] H. Ma, S. Qu, Z. Xu, and J. Wang, Opt. Express **16**, 15449 (2008).
[10] H. Chen and C. T. Chan, Appl. Phys. Lett. **91**, 183518 (2007).
[11] S. A. Cummer, B. I. Popa, D. Schurig, D. R. Smith, J. B. Pendry, M. Rahm, and A. F. Starr, Phys. Rev. Lett. **100**, 024301 (2008).
[12] D. Torrent and J. Sanchez-Dehesa, New J. Phys. **10**, 063015 (2008).
[13] Y. Cheng, F. Yang, J. Y. Xu, and X. J. Liua, Appl. Phys. Lett. **92**, 151913 (2008).
[14] A. N. Norris, Proc. R. Soc. London, Ser. A **464**, 2411 (2008).

[15]S. Zhang, C. Xia, and N. Fang, Phys. Rev. Lett. **106**, 024301 (2011).
[16]J. Li and J. B. Pendry, Phys. Rev. Lett. **101**, 203901 (2008).
[17]R. Liu, C. Ji, J. J. Mock, J. Y. Chin, T. J. Cui, and D. R. Smith, Science **323**, 366 (2009).
[18]J. Valentine, J. Li, T. Zentgraf, G. Bartal, and X. Zhang, Nature Mater. **8**, 568 (2009).
[19]L. H. Gabrielli, J. Cardenas, C. B. Poitras, and M. Lipson, Nat. Photonics **3**, 461 (2009).
[20]T. Ergin, N. Stenger, P. Brenner, J. B. Pendry, and M. Wegener, Science **328**, 337 (2010).
[21]G. W. Milton, M. Briane, and J. R. Willis, New J. Phys. **8**, 248 (2006).
[22]Y. Urzhumov, F. Ghezzo, J. Hunt, and D. R. Smith, New J. Phys. **12**, 073014 (2010).
[23]W. Li, J. Guan, Z. Sun, W. Wang, and Q. Zhang, Opt. Express **17**, 23410 (2009).
[24]J. Zhang, Y. Luo, and N. A. Mortensen, Opt. Express **18**, 3864 (2009).
[25]W. Zhu, C. Ding, and X. Zhao, Appl. Phys. Lett. **97**, 131902 (2010).
[26]D. Torrent and J. Sanchez-Dehesa, New J. Phys. **10**, 023004 (2008).
[27]B. I. Popa and S. A. Cummer, Phys. Rev. B **80**, 174303 (2009).
[28]J. B. Pendry and J. Li, New J. Phys. **10**, 115032 (2008).
[29]M. F. Ashby, A. G. Evans, N. A. Fleck, L. J. Gibson, J. W. Hutchinson, and H. N. G. Wadley, *Metal Foams: A Design Guide* (Butterworth-Heinemann, Boston, 2000).
[30]Duocell Silicon Carbide Foam Produced by Materials and Aerospace Corporation (see [http://www.ergaerospace.com/foamproperties/sicproperties.htm]).